

## PEGylated long-circulating liposomes deliver homoharringtonine to suppress multiple myeloma cancer stem cells

Miao Li<sup>1</sup>, Fangfang Shi<sup>1</sup>, Xiong Fei<sup>2</sup>, Songyan Wu<sup>1</sup>, Di Wu<sup>1</sup>, Meng pan<sup>1</sup>, Shouhua Luo<sup>2</sup>, Ning Gu<sup>2</sup> and Jun Dou<sup>1</sup>

<sup>1</sup>Department of Pathogenic Biology and Immunology, School of Medicine, Southeast University, Nanjing 210009, China; <sup>2</sup>School of Biological Science & Medical Engineering, Southeast University, Nanjing 210096, China

Miao Li and Fangfang Shi contributed equally to the work.

Corresponding authors: Jun Dou. Email: njdoujun@seu.edu.cn; Ning Gu. Email: guning@seu.edu.cn

### Impact statement

Multiple myeloma (MM) remains largely incurable until now. One of the main reasons is that there are cancer stem cells (CSCs) in MM, which are responsible for MM's drug resistance and relapse. In this study, we wanted to extend our previous investigation<sup>22</sup> that whether we developed the LCL-HHT-H-PEG formulation have an inhibitory effect on MM CD138<sup>+</sup>CD34<sup>+</sup> CSCs in MM CSC engrafted NOD/SCID mouse model. Our data from the present study have demonstrated the therapeutic effect of LCL-HHT-H-PEG on MM-bearing mouse model. The study represents the first attempt to demonstrate that the LCL-HHT-H-PEG formulation is available for treatment MM patients in clinic. Therefore, this finding is important and deserves publication in *Experimental Biology and Medicine*.

### Abstract

The goal of this investigation was to evaluate the inhibiting effect of high proportion poly-ethyleneglycol of long-circulating homoharringtonine liposomes on RPMI8226 multiple myeloma cancer stem cells. The CD138<sup>+</sup>CD34<sup>+</sup> multiple myeloma cancer stem cells isolated from RPMI8226 cell line using magnetic activated cell sorting system were, respectively, incubated with the optimized formulation of polyethyleneglycol of long-circulating homoharringtonine liposomes and the homoharringtonine *in vitro*, and the multiple myeloma cancer stem cell proliferation, colony formation, and cell cycle were analyzed. The inhibition of the multiple myeloma CD138<sup>+</sup>CD34<sup>+</sup> cancer stem cell growth was investigated in non-obese-diabetic/severe-combined-immunodeficiency mice that were implanted with multiple myeloma RPMI 8226 cancer stem cells and treated with the LCL-HHT-H-PEG. The results showed that the polyethyleneglycol of long-circulating homoharringtonine liposomes significantly inhibited MM cancer stem cell proliferation, colony formation, and induced cancer stem cell apoptosis *in vitro* as well as MM cancer stem cell growth in non-obese-diabetic/severe-combined-immunodeficiency mice compared with the homoharringtonine.

In addition, the mouse bone mineral density and the red blood cell count were significantly increased in polyethyleneglycol of long-circulating homoharringtonine liposomes group. In conclusion, the data demonstrated that the developed polyethyleneglycol of long-circulating homoharringtonine liposomes formulation may serve as an efficient therapeutic drug for suppressing CD138<sup>+</sup>CD34<sup>+</sup> multiple myeloma cancer stem cell growth by inducing cancer stem cell apoptosis in non-obese-diabetic/severe-combined-immunodeficiency mouse model.

**Keywords:** Multiple myeloma, cancer stem cells, homoharringtonine, long-circulating liposomes, polyethyleneglycol

*Experimental Biology and Medicine* 2017; 242: 996–1004. DOI: 10.1177/1535370216685008

### Introduction

Multiple myeloma (MM), the second most common hematological malignancy, accounts for approximately 10% of hematologic cancers.<sup>1,2</sup> MM patients clinically result in anemia, immunodeficiency, renal insufficiency, hypercalcemia, and an increase of infection risk.<sup>2,3</sup> Although the recent advances were made in the treatment of MM patients with the introduction of the novel agents such as bortezomib (proteasome inhibitor), thalidomide, and lenalidomide (immunomodulatory drugs), which has significantly improved patient's response rate and survival, most MM

patients eventually relapse and succumb to the disease that still remains incurable.<sup>4–6</sup>

It was known that the tumor-initiating population and/or CSCs are distinguished by their ability to produce tumors, and are responsible for maintaining the pull of residual disease, eventual chemo-resistance, and recurrence in MM patients.<sup>7–10</sup> Despite the theory of MM CSCs proposed for the drug resistance in MM patients, how to target MM CSCs for solving the resistant problem has not been properly defined yet.<sup>6,11</sup> Therefore, there is an unmet need for new therapies to lengthen survival of MM patients.<sup>12,13</sup> Recently, a trio of United States Food and Drug

Administration drug approvals for MM, including two immunotherapies (daratumumab, elotuzumab) and an oral proteasome inhibitor (ixazomib) have suddenly broadened oncologists' options for treatment of MM patients, suggesting that therapeutic approaches to this disease focus on discovering a novel therapeutic drugs to enhance efficacy of treating MM patients.<sup>14</sup>

Homoharringtonine (HHT) isolated from the Cephalotaxus evergreen tree has been widely used in traditional Chinese medicine for treatment of a variety of hematologic malignancies, and also approved by the Food and Drug Administration of United States for treating patients within acute and chronic myeloid lymphoma.<sup>15-17</sup> However, HHT may induce unanticipated side effects in the gastrointestinal tract, which limits its wide clinical utility.<sup>15</sup> Given the growing use of liposome encapsulation of anticancer drugs to alter their pharmacokinetics and distribution *in vivo*, these drugs have decreased the toxicity and increased the drug efficacy.<sup>18-20</sup> Accumulating evidence has showed that the long-circulating dose-independent liposome formulations containing polyethyleneglycol (PEG) on the surface of liposomes has been approved for treatment of the different tumors.<sup>21-23</sup> In our previous study,<sup>22</sup> we developed the high proportion PEGylated long-circulating liposomes containing HHT (LCL-HHT-H-PEG) to have evaluated the therapeutic effects on MM RPMI8226 cells *in vitro* and *in vivo*, indicating encouraging results of inhibitory MM growth compared with general liposome-encapsulated-HHT, low proportion PEG of long-circulating HHT liposomes, and micelle-HHT. In this study, we wanted to extend the investigation that whether the LCL-HHT-H-PEG have an inhibitory effect on MM RPMI8226 CD138<sup>+</sup>CD34<sup>+</sup>CSCs. From the present study, our results indicated that, compared with the control HHT, the LCL-HHT-H-PEG formulation showed a significant suppression of MM CSC proliferation *in vitro* and MM CSC growth in non-obese-diabetic/severe-combined-immunodeficiency (NOD/SCID) mice injected with MM RPMI8226 CD138<sup>+</sup>CD34<sup>+</sup>CSCs. The data demonstrated that the LCL-HHT-H-PEG formulation might be worth further exploration for the treatment of MM patients by targeting CD138<sup>+</sup>CD34<sup>+</sup>CSCs.

## Materials and methods

### Cells

Human MM RPMI 8226 cells were purchased from the Institute of Basic Medical Sciences Chinese Academy, People's Republic of China. Cells were cultured in complete medium consisting of RPMI 1640, 2 mM L-glutamine, 100 U/mL penicillin, 100 µg/mL streptomycin, and 10% fetal bovine serum at 37°C in a humidified incubator containing 5% CO<sub>2</sub>.

### NOD/SCID mice

NOD/SCID mice at five to six weeks of age with 16-18 g in weight were purchased from Slac laboratory animal center, Shanghai, China. All the mice were maintained in a pathogen-free facility that has a 12-h light/dark cycle

and relative humidity ranged from 40% to 50% at 22°C. All the animal experiments were performed in compliance with the Guidelines of the Animal Research Ethics Board of Southeast University. Full details of approval of the study can be found in the approval ID: 20080925.

### Main materials

Mouse anti-human CD138 and CD34 microbead monoclonal antibody were purchased from Miltenyi Biotec (Bergisch Gladbach, Germany). HHT was purchased from Dalian Meilun Biotech Co., Ltd of China. The annexin V-PE/7-AAD apoptosis assay kit (KGA1017) was purchased from Nanjing KeyGen Biotech. Co., Ltd. 1,2-distearoyl-sn-glycero-3-phosphoethanolamine-N-[methoxy (polyethylene glycol)-2000]-biotin (DSPE-PEG 2000-Biotin) and 25-NBD-cholesterol were purchased from Avanti Polar Lipids, Inc. Matrigel was purchased from BD Biosciences (USA). Cell cycle and JC-1 apoptosis detection kit were procured from Keygen Biotech of China. All other chemicals were commercially available and analytical grade.

### Developing of LCL-HHT-H-PEG formulation

Firstly, HHT formulation was prepared as follow: 206.24 mg of natural phospholipids, 10.15 mg of cholesterol, 20.42 mg of HHT, and 100 mg of DSPE-PEG2000 were synchronously dissolved in 1 ml of ethanol with ultrasound. This solution was added in 20 ml pure water slowly drop by drop with vortex to get the mixture. Liposome suspension was obtained after removing the organic solvent from the mixture. The suspension was concentrated to reduce the size of liposomes with probe ultrasound, and then the suspension was freeze dried with 1.2 ml liposome and 1.2 ml (100 mg/ml) sucrose solution in each vial after determination of content. Finally, we got the high proportion PEG of long-circulating HHT liposomes (1.006 mg/vial), and named it for LCL-HHT-H-PEG.<sup>20-22</sup>

### Preparation of CD138<sup>+</sup>CD34<sup>+</sup> MM CSCs

CD138<sup>+</sup> cells were isolated from human MM RPMI 8226 cells using mouse antihuman CD138 monoclonal antibody coupled to magnetic microbeads (Miltenyi Biotec, Germany) followed by magnetic column selection, using immune magnetic activated cell sorting (Miltenyi Biotec, Germany). Resulting cells were additionally depleted of normal hematopoietic progenitors by using mouse antihuman CD34 antibody (Miltenyi Biotec, Germany).<sup>7,24,25</sup> The CD138<sup>+</sup>CD34<sup>+</sup> cells were analyzed by flow cytometer (FCM, FACS Caliber, BD, USA). We named CD138<sup>+</sup>CD34<sup>+</sup> cells in human MM RPMI 8226 cell line for the MM stem-like cells (MM CSCs) as described in our previous reports.<sup>11,26</sup>

### Assay of colony formation in soft agar media

The assay protocol of colony formation was described in our previous reports.<sup>24,25</sup> Briefly,  $2 \times 10^2$  CD138<sup>+</sup>CD34<sup>+</sup> MM CSC suspensions were resuspended in 0.8 mL growth media containing 0.3% low melting temperature agarose (Promega, Madison, WI, USA) and the

LCL-HHT-H-PEG (40 ng/0.8 ml) or HHT (40 ng/0.8 ml) or LCL-H-PEG (40 ng/0.8 ml, high proportion PEGylated long-circulating liposomes without HHT) was plated in triplicate on 24-well plate over a base layer of 0.8 mL growth media containing 0.6% low melting temperature agarose. The plates were incubated for two weeks until colonies were formed. Colony diameters larger than 75  $\mu$ m or colony cells more than 50 cells were then counted as one positive colony visualized by light a microscope (10  $\times$  10).

### Cell cycle of MM CSCs analyzed by FCM

In cell cycle assay,  $1 \times 10^6$  CD138<sup>+</sup>CD34<sup>+</sup>MM CSCs were incubated with the LCL-HHT-H-PEG formulation or HHT or LCL-H-PEG each well (40 ng/ml) at 37°C in 5% CO<sub>2</sub> for 72 h, and fixed overnight with 70% (w/v) ice-cold ethanol. Cells then were resuspended in 1 mL of PBS containing 40  $\mu$ g/mL Annexin V/PI and 500 U/mL RNase A. Following incubation for 30 min in the dark at room temperature, cells were analyzed by FCM using the system modfit software. The PI fluorescence signal peak versus the integral was used to discriminate G2-M cells from G0 to G1 doublets by using cell cycle and JC-1 apoptosis detection kit.<sup>27,28</sup>

### Animal experiments

CD138<sup>+</sup>CD34<sup>+</sup>MM CSCs ( $4 \times 10^6$ ) were mixed with matrigel (100  $\mu$ L in volume) and injected subcutaneously into the dorsal side in NOD/SCID mice. The palpable tumors at the injection sites were examined after around 12 days, and these MM-bearing mice were randomly divided into HHT and LCL-HHT-H-PEG groups. Three days after MM-bearing mice were established, the tumor area in each mouse was locally treated with 150 mg/kg HHT or 150 mg/kg LCL-HHT-H-PEG (100  $\mu$ L in volume), in total of 10 times with three-day intervals between the treatments. Three mice/group were used in the study, and the experiment was repeated twice. The tumor growth in NOD/SCID mice was monitored once three days for tumor volume. The general health indicators of mice, such as overall behavior, feeding, body weight and appearance of fur after treatment, were also monitored. The endpoint for this study was the diameter of tumor  $\geq 15$  mm, and then mice were anesthetized with phenobarbital sodium and executed. Mouse tumor tissues, bones, blood, and spleens were collected for further analysis.<sup>11</sup>

### Bone lesion analysis

MM-bearing mice were anesthetized with phenobarbital sodium and executed by cervical dislocation 30 days after treatment. The femurs, humerus, and vertebra were, respectively, removed for detection of lytic bone lesions by microcomputed to micrography (Micro-CT, MCT-1108, China), and the parameters of voltage 45 mV and electric current 90 mA were used in the assay.<sup>24,29,30</sup>

### Western blot

$1 \times 10^6$  tumor tissue cells from the MM-bearing mice treated with LCL-HHT-H-PEG or HHT were collected and lysed in

a protein extraction buffer (Novagen, WI, USA) according to the manufacturer protocol. Western blot was performed after a 10% SDS-polyacrylamide gel electrophoresis. The membrane was blocked with a blocking solution 30 min on a rotary shaker, then washed twice with a washing solution and subsequently incubated with a rabbit antihuman caspase-8, caspase-9, caspase-3, and Beta-actin (Bioworld, MN) for 1 h, respectively. The following steps were performed according to the Kit's protocol.<sup>31,32</sup>

### Statistical analysis

Spss17.0 and Graphpad Prism 5.0 were used for data analysis. Values of interest were presented as the mean plus or minus standard deviation. Statistical analysis was performed using the Student's *t*-test method. Differences were considered statistically significant if *P* values < 0.05.

## Results

### Properties of the LCL-HHT-H-PEG formulation

The properties of LCL-HHT-H-PEG were described in our previous report.<sup>22</sup> Figure 1 shows that the different components in formulations of LCL-HHT-H-PEG, which are Cholesterol (a), PEG (b), phospholipids (c), Liposomes-phospholipids (d), HHT (e), LCL-H-PEG (f), and LCL-HHT-H-PEG (g) in order. It was found that the LCL-HHT-H-PEG was maintained in the spherical shape, and there were some floccules in the hollow carries, and no rupture of the capsule wall, and that the LCL-HHT-H-PEG formulations were well demarcated, suggesting that a typical vesicle structure had been formed.

### In vitro inhibitive efficacy of the LCL-HHT-H-PEG on proliferation, clone formation, and cell cycle of MM CSCs

In our previous study,<sup>22</sup> we found that the developed LCL-HHT-H-PEG formulation had significant inhibitive effects on MM RPMI 8226 cell growth by inhibition of clone formation and induction of cell apoptosis *in vitro* compared with other control formulations including general liposome-encapsulated-HHT, low proportion PEG of long-circulating HHT liposomes, and micelle-HHT. In this study, we sought to know if the LCL-HHT-H-PEG would work on MM RPMI 8226 CSCs. We first observed the proliferation ability when MM RPMI 8226 CSCs were incubated with the LCL-HHT-H-PEG formulation for 24, 48, and 72 h, respectively. Figure 2(a) shows that inhibition of MM CSC proliferation was significantly increased in LCL-HHT-H-PEG group compared with the HHT group (*P* < 0.05) or LCL-H-PEG group (*P* < 0.01) when the incubation lasted 72 h. However, we found that there was no significant difference between the LCL-HHT-H-PEG and HHT groups in inhibition of MM CSC proliferation in 24 or 48 h, which suggested the LCL-HHT-H-PEG formulation has lasted inhibitive effect on MM CSC proliferation due to slow release of HHT from the LCL-HHT-H-PEG. Figure 2(b) indicates that clone formation rate was significantly lower in LCL-HHT-H-PEG group than that of HHT group ( $4.9 \pm 0.79\%$  vs.  $9.6 \pm 0.28\%$ , *P* < 0.05) or LCL-H-PEG



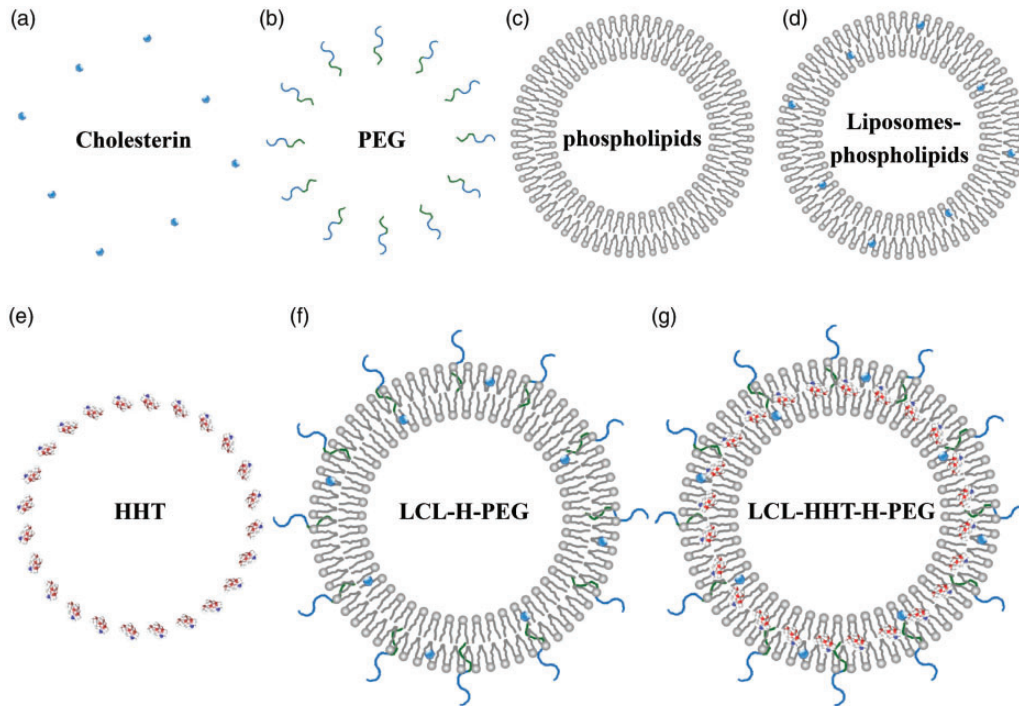


**Figure 1** Illustration of LCL-HHT-H-PEG formulation. (a) Cholesterolin. (b) PEG. (c) Phospholipids. (d) Liposomes-phospholipids. (e) HHT. (f) LCL-H-PEG. (g) High proportion PEG of long-circulating HHT liposomes (LCL-HHT-H-PEG). (A color version of this figure is available in the online journal.)

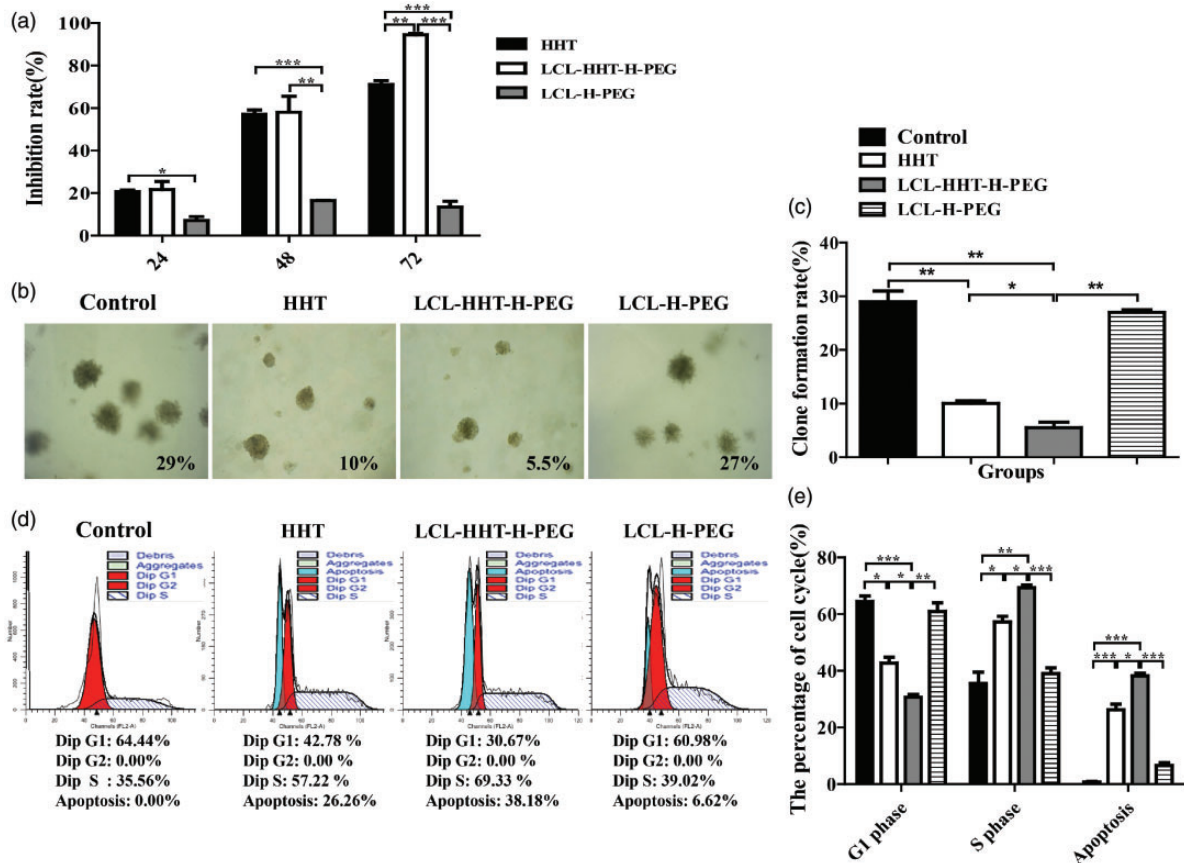


**Figure 2** Inhibitive effects of LCL-HHT-H-PEG on MM CD138<sup>+</sup>CD34<sup>-</sup> CSCs *in vitro*. (a) Proliferative inhibition assay. (b) Clone formation rate of MM CD138<sup>+</sup>CD34<sup>-</sup> CSCs. (c) Quantification of clone formation rate. (d) MM CSC apoptosis, G1 and S phases in cell cycle analyzed by FCM as described in the section of Materials and methods. (e) Quantification analysis of percentage of MM CSC cycle. \**P* < 0.05, \*\**P* < 0.01, and \*\*\**P* < 0.005. (A color version of this figure is available in the online journal.)

group ( $4.9 \pm 0.79\%$  vs.  $27.6 \pm 0.15\%$ / $29.1 \pm 0.98\%$ ,  $P < 0.001$ ), shown in Figure 2(c), after two week culture. The cell cycles in Figure 2(d) exhibited that apoptosis rate was significantly increased in LCL-HHT-H-PEG group compared with in LCL-H-PEG group ( $39 \pm 0.28\%$  vs.  $7.2 \pm 0.19\%$ ,  $P < 0.001$ ) or HHT group ( $39 \pm 0.28\%$  vs.  $23.2 \pm 1.16\%$ ,  $P < 0.05$ ), strongly suggesting LCL-HHT-H-PEG induced MM CSC apoptosis *in vitro*. Additionally, the difference of G1 and S phases was statistically significant between the LCL-HHT-H-PEG group and the other groups as is shown in Figure 2(e).

### In vivo inhibitive efficacy of LCL-HHT-H-PEG on MMSC growth in mice

We next attempted to demonstrate whether the developed LCL-HHT-H-PEG formulation could translate *in vitro* inhibitive effect on MM CSCs into *in vivo* inhibitive effect on MM CSC growth in mice. For this reason, we established the MM xenograft model by subcutaneous injection of human MM RPMI 8226 CSCs into the NOD/SCID mice. All the injected mice generated MM xenografts 12 days after injection of  $4 \times 10^6$  MM CSCs per mouse; the MM-bearing mice were, respectively, treated with

LCL-HHT-H-PEG and HHT on day 15 (the initiation of treatment). Figure 3(a) indicates the dynamic curves of mouse weight. From the day 15 to the day 42 (the termination of treatment), the weight loss was around 4.6% in the HHT-treated mice compared with the LCL-HHT-H-PEG-treated mice, and the difference was statistically significant ( $P < 0.05$ ), suggesting the toxicity of HHT to mice was more serious than that of LCL-HHT-H-PEG. Figure 3(b) gives the pictures of MM-bearing NOD/SCID mice after the mice were treated with the LCL-HHT-H-PEG formulation or the HHT. Figure 3(c) shows the tumor sizes that were stripped from the mice after the termination of treatment. The quantification analysis of tumor sizes was shown in Figure 3(d). It was found that tumor size was smaller in LCL-HHT-H-PEG-treated mice than that of HHT-treated mice. The difference was statistically significant ( $P < 0.05$ ). The survival of MM-bearing mice treated with the HHT was 36, 39, and 43 days, and the mean survival was of 39.3 days. In contrast, only one of the three MM-bearing mice in the LCL-HHT-H-PEG group was died on day 39, and no death was found in the remaining two mice until 45 days into the observation (Figure 3(e)). From this therapeutic experiment results, we concluded that the LCL-HHT-H-PEG have

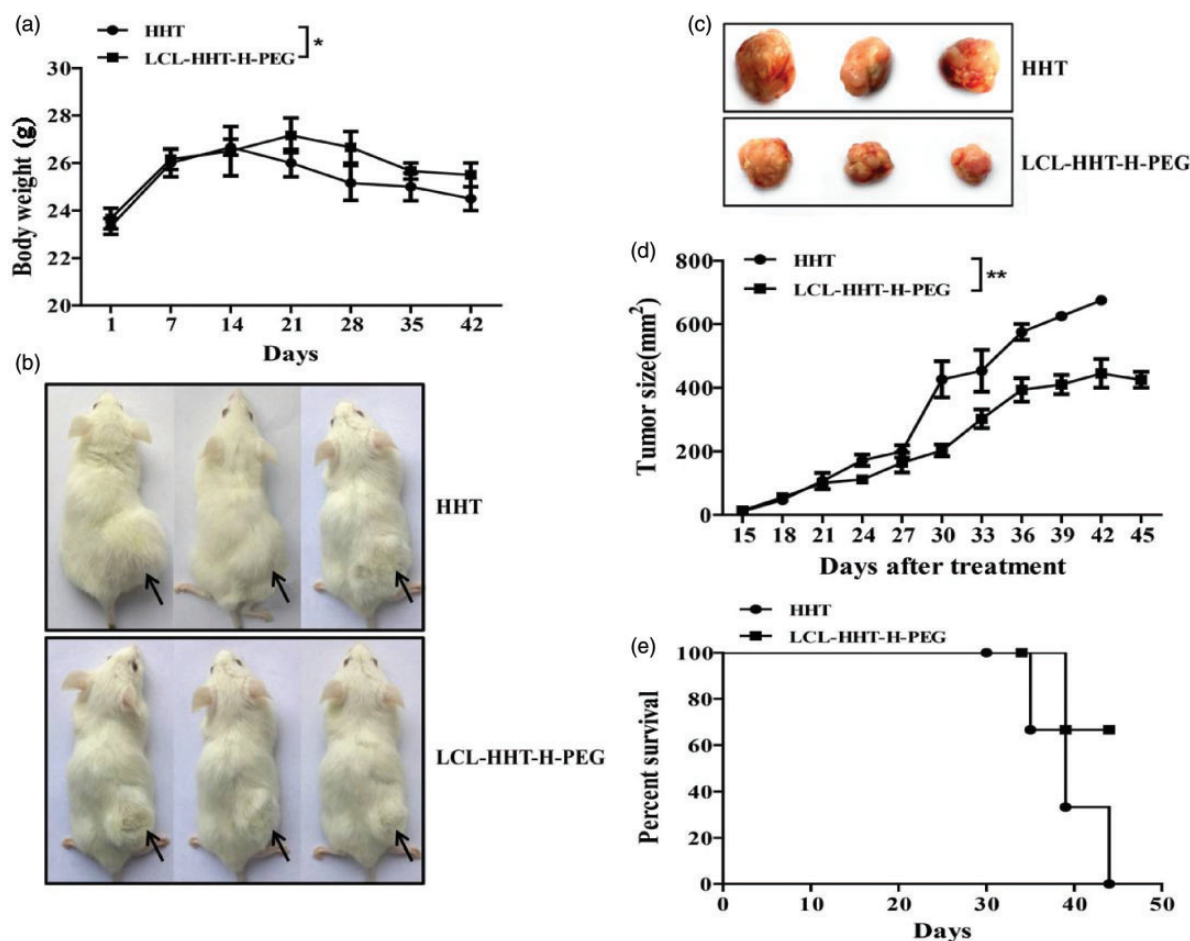


**Figure 3** Therapeutic effects of LCL-HHT-H-PEG on MM CD138<sup>+</sup>CD34<sup>-</sup> CSCs *in vivo*. (a) Dynamic curves of NOD/SCID weight. (b) Images of MM-bearing mice injected with MM CD138<sup>+</sup>CD34<sup>-</sup> CSCs on day 30. (c) Images of tumor sizes after the mice were treated with the HHT or LCL-HHT-H-PEG formulation once three-day with total of 10 times as described in the section of Materials and methods. (d) Quantification of tumor sizes. (e) MM-bearing mice's survival. \* $P < 0.05$  and \*\* $P < 0.01$ . (A color version of this figure is available in the online journal.)

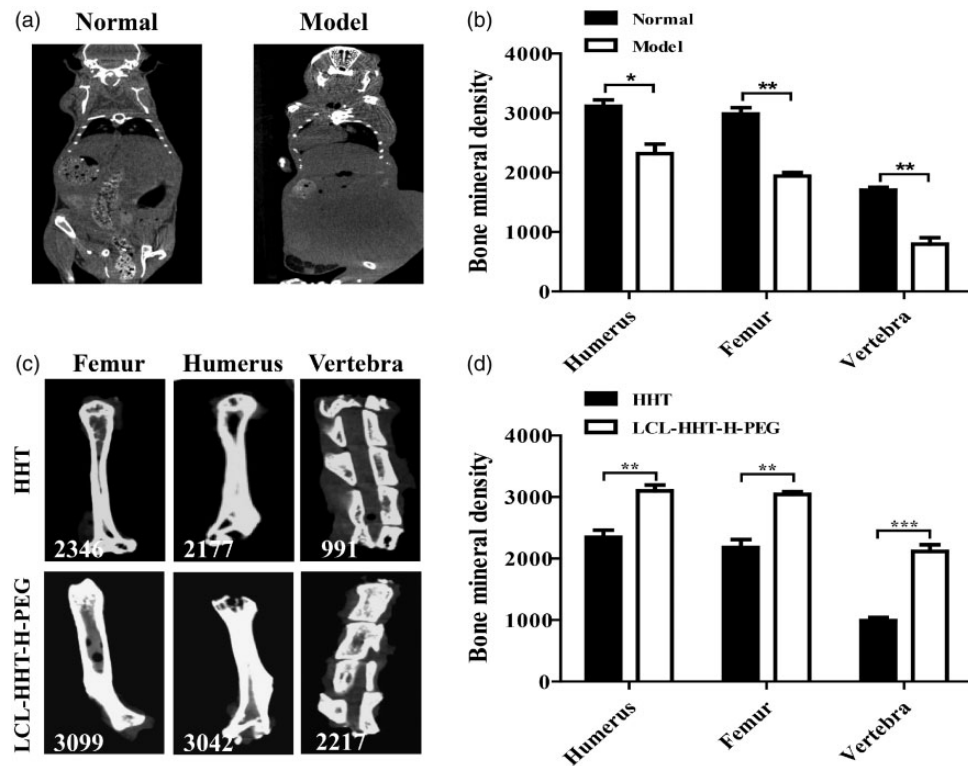


**Figure 4** Bone mineral density was increased in MM CD138<sup>+</sup>CD34<sup>+</sup> CSC xenograft mice treated with LCL-HHT-H-PEG formulation. (a) Bone mineral density in normal mouse and model mouse injected with MM CD138<sup>+</sup>CD34<sup>+</sup> CSCs scanned by *in vivo* Micro-CT on Day 30. (b) Quantification of whole mouse bone mineral density. (c) A representative clinical images of NOD/SCID mice treated with the HHT or LCL-HHT-H-PEG formulation once three-day with total of 10 times. (d) Quantification of whole mouse bone mineral density. \* $P < 0.05$ , \*\* $P < 0.01$ , and \*\*\* $P < 0.005$

stronger therapeutic effect than that of HHT in MM xenograft mouse model.

LCL-HHT-H-PEG increases the mouse bone mineral density in MM-bearing mice. Since the LCL-HHT-H-PEG formulation was efficient in inhibition of RPMI 8226 MM CSC growth in mice, we wanted to further know whether this effect would have relieved the lytic bone lesions in MM-bearing mouse model. Figure 4(a) shows the representative clinical pictures, scanned by *in vivo* Micro-CT imaging in normal mice and RPMI 8226 MM CSC xenograft mice. Figure 4(b) indicates the bone mineral density (femurs, humerus, and vertebra) in two group mice without treatment. After mice were respectively treated with LCL-HHT-H-PEG and HHT, the femurs, humerus, and vertebra were successively stripped from the treated mice; the bone mineral density was scanned, and images were shown in Figure 4(c), in which the numbers represent the account of mouse bone mineral density. We found that the LCL-HHT-H-PEG formulation significantly increased the bone mineral density and ameliorated lytic bone lesions compared with the control HHT in the MM CSC xenograft mice. The difference was statistically significant as shown in Figure 4(d). The results of mouse bone mineral density demonstrated that the application of LCL-HHT-H-PEG formulation to RPMI 8226 MM CSC xenograft NOD-SCID mice significantly relieved the lytic bone lesions and increased mouse bone mineral density compared with the mice treated with the HHT.

#### **LCL-HHT-H-PEG induces the apoptosis of MM cells *in vivo* and increases the index of spleen and RBC count**

Next, we sought to know the possible mechanism of the LCL-HHT-H-PEG treatment of MM-bearing mice. The MM tissues were isolated from the treated mice that were injected with MM CSCs. The MM tissue suspensions were prepared for Western blot assay. Figure 5(a) showed that the expression of caspase-3 was significantly increased in the MM tissues from the mice treated with LCL-HHT-H-PEG group compared with the HHT group, and the caspase-3 activity was also true, which was reflected in high cleaved caspase-3 expression. The result from caspase-8 expression in MM tissues from the mice treated with LCL-HHT-H-PEG group indicated a similar one as did caspase-8 expression in HHT group, and there is no statistically significant between the groups ( $P > 0.05$ ); but caspase-9 expression was increased in the LCL-HHT-H-PEG group. Statistical analysis of caspase expressive changes in MM tissues is shown in Figure 5(b). In addition, we found that the representative clinical spleen images in Figure 5(c) showed the spleen index was significantly increased in LCL-HHT-H-PEG-treated mice compared to HHT-treated mice, which was statistically significant ( $P < 0.05$ ) in Figure 5(d). Similarly, the index of RBC was also significantly increased in LCL-HHT-H-PEG-treated mice compared to HHT-treated mice, and the difference was statistically significant ( $P < 0.05$ ) (Figure 5(e)).



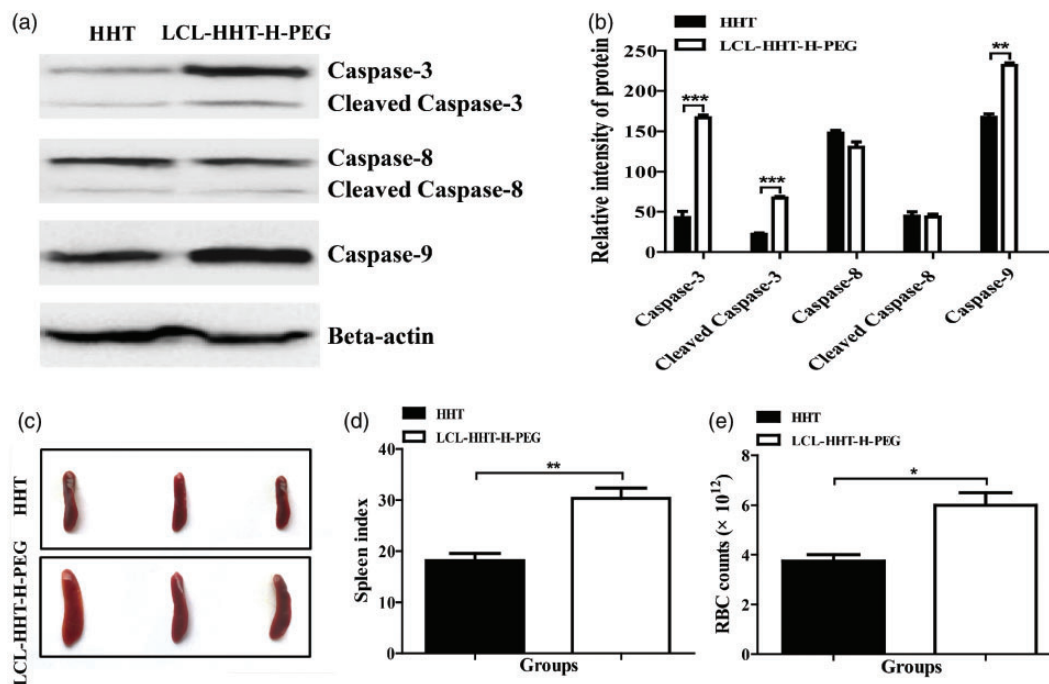


**Figure 5** Detection of the expression of apoptotic molecules and the index of spleen and RBC count. (a) The expression of apoptotic molecules in MM tissues of NOD/SCID mice analyzed by Western blot assay. (b) Quantification of the expression of apoptotic molecules. (c) Images of spleen sizes. (d) Quantification of the spleen index. (e) Quantification of the RBC count as described in the section of Materials and Methods. \* $P < 0.05$ , \*\* $P < 0.01$ , and \*\*\* $P < 0.005$ . (A color version of this figure is available in the online journal.)

It is known that caspase-8 and caspase-9 are activated by the death receptor signaling pathway and the mitochondrial signaling pathway during apoptosis in order, whereas caspase-3 is a common effector of both signaling pathways.<sup>33,34</sup> Therefore, we speculate that the LCL-HHT-H-PEG might induce MM CSC apoptosis via mitochondrial apoptotic pathway. This was because the LCL-HHT-H-PEG formulation enhanced the expression of the initiator caspase-9 and the executioner caspase-3, which led to MM cell apoptosis.

## Discussion

Emerging evidence supports the view that a subpopulation of MM cells that are highly resistant to conventional cancer therapies shares certain CSC features. The CSCs are thought to be responsible for eventual chemoresistances and relapse in MM patients.<sup>7,8,11</sup> Therefore, development of effective targeted therapeutic agents is necessary to control the disease.

In current study, we expanded our previous study by using developed the LCL-HHT-H-PEG to investigate whether this novel drug would have the inhibitory effects on MM RPMI8226 CSCs *in vitro* and *in vivo*. We have found that the LCL-HHT-H-PEG formulation not only had obvious efficacy of inhibiting clone formation and inducing apoptosis of MM RPMI8226 cells,<sup>22</sup> but also had similar effects on inhibiting MM CD138<sup>+</sup>CD34<sup>+</sup>CSC progression that was shown in suppressing MM CSC proliferation, clone formation, and promoting cell apoptosis compared with the HHT *in vitro*. Importantly, *in vivo* MM murine

model established by subcutaneous injection of MM CD138<sup>+</sup>CD34<sup>+</sup>CSCs, the LCL-HHT-H-PEG formulation showed a stronger therapeutic activity than that of HHT, which was reflected in inhibition of MM growth observed by MM-bearing mice's survival, and remission of the lytic bone lesions detected by micro-computer tomography scanning. In addition, the LCL-HHT-H-PEG formulation increased the red blood cell count and the spleen index, suggesting the improvement of MM mice's clinic signs and increase of MM-bearing mice's ability of anti-infections. The strong therapeutic activity of LCL-HHT-H-PEG is apparently associated with its strong activity to induce MM tissue cell apoptosis, which was demonstrated by Western blot analysis. These comprehensive effects of suppressing MM CSC growth in MM-bearing mice treated with the LCL-HHT-H-PEG were more obvious than that of HHT. It is known that PEG-coated liposomes displayed lower uptake by the phagocytes and longer circulation time than liposomes without PEG coating.<sup>31,32,35</sup> We guess that PEG-coated liposomes formed the bilayer in the LCL-HHT-H-PEG and made it more rigid and more stability, which might safeguard LCL-HHT-H-PEG from the degradation by biological activity materials or enzyme digestion. Consequently, the LCL-HHT-H-PEG formulation has stronger bioavailability in inhibiting MM CSC growth with decrease of chemotherapeutic side effects than that of HHT without PEG-coated liposomes. Although the above-mentioned findings are encouraging, however, further investigation of the molecular mechanisms of suppressing MM RPMI8226 CSC growth in mice treated with

LCL-HHT-H-PEG formulation still is a necessary for this drug treatment of MM disease.

In summary, the data from the present study have demonstrated the therapeutic effect of LCL-HHT-H-PEG on MM-bearing NOD/SCID mouse model. To our knowledge, this investigation is the first to report the therapeutic efficacy of LCL-HHT-H-PEG formulation in MM CD138<sup>+</sup>CD34<sup>+</sup>CSC xenograft mice. The novel agent may be regarded as a promising drug for treatment of MM patients in clinical trials.

**Authors' contributions:** ML, FFS, SYW, and DW conducted the experiments, ML, FX, SYW, MP, SHL, and JD analyzed the data, ML, SYW, NG, and JD wrote the manuscript or revised it for important intellectual content. All authors read and approved the final manuscript.

## ACKNOWLEDGMENTS

The study was supported by the National Natural Science Foundation of China (No. 81572887, No.81473160), and partly supported by the Fundamental Research Funds for the Central Universities, Southeast University (3290005416) as well as partly supported by the Collaborative Innovation Center of Suzhou NanoScience and Technology.

## DECLARATION OF CONFLICTING INTERESTS

The author(s) declared no potential conflicts of interest with respect to the research, authorship, and/or publication of this article.

## REFERENCES

- Saini N, Mahindra A. Therapeutic strategies for the treatment of multiple myeloma. *Discov Med* 2013;**15**:251–8
- Dou J, He X, Liu YJ, Huang Z H, Yang C P, Shi F. Targeted therapeutic effect of anti-ABCG2 antibody combined with nano silver and vincristine on mouse myeloma cancer stem cells. *J Nanopart Res* 2013;**15**:2127
- Borrello I. Can we change the disease biology of multiple myeloma? *Leuk Res* 2012;**36**(Suppl 1): S3–12
- Atanackovic D, Hildebrandt Y, Templin J, Cao Y, Keller C, Panse J. Role of interleukin 16 in multiple myeloma. *J Natl Cancer Inst* 2012;**104**:1005–20
- Thirukkumaran CM, Shi ZQ, Luijer J, Kopciuk K, Gao H, Bahlis NJ. Reovirus as a viable therapeutic option for the treatment of multiple myeloma. *Clin Cancer Res* 2012;**18**: 4962–72
- Abe M, Harada T, Matsumoto T. Concise review: Defining and targeting myeloma stem cell-like cells. *Stem Cells* 2014;**32**:1067–73
- Matsui W, Huff CA, Wang Q. Characterization of clonogenic multiple myeloma cells. *Blood* 2004;**103**:2332–6
- Dou J, Li Y, Zhao F, Hu W, Wen P, Tang Q. Identification of tumor stem-like cells in a mouse myeloma cell line. *Cell Mol Biol* 2009;**55**(Suppl): OL1151–60
- Matsui W. Perspective: A model disease. *Nature* 2011;**480**: S58
- Al-Hajj M, Wicha MS, Benito-Hernandez A, Clarke MF. Prospective identification of tumorigenic breast cancer cells. *Proc Natl Acad Sci USA* 2003;**100**:3983–8
- Yang C, Xiong F, Dou J, Xue J, Zhan X, Shi F. Target therapy of multiple myeloma by PTX-NPs and ABCG2 antibody in a mouse xenograft model. *Oncotarget* 2015;**6**:27714–24
- Lonial S, Durie B, Palumbo A, Miguel JS. Monoclonal antibodies in the treatment of multiple myeloma: Current status and future perspectives. *Leukemia* 2016;**30**:526–35
- Maiso P, Huynh D, Moschetta M, Sacco A, Aljawai Y, Mishima Y. Metabolic signature identifies novel targets for drug resistance in multiple myeloma. *Cancer Res* 2015;**75**:2071–82
- Ratner M. FDA approves three different multiple myeloma drugs in one month. *Nat Biotechnol* 2016;**34**:126
- Ustuwani A O, Griffiths EA, Wang ES, Wetzler M. Omacetaxine mepe-succinate in chronic myeloid leukemia. *Expert Opin Pharmacother* 2014;**15**:2397–2405
- Philipp S, Sosna J, Plenge J, Kalthoff H, Adam D. Homoharringtonine, a clinically approved anti-leukemia drug, sensitizes tumor cells for TRAIL-induced necroptosis. *Cell Commun Signal* 2015;**13**:25
- Watairi A, Hashegawa M, Yagi K, Kondoh M. Homoharringtonine increases intestinal epithelial permeability by modulating specific claudin isoforms in Caco-2 cell monolayers. *Eur J Pharm Biopharm* 2015;**89**:232–8
- Papahadjopoulos D, Allen TM, Gabizon A, Mayhew E, Matthay K, Huang SK. Sterically stabilized liposomes: Improvements in pharmacokinetics and antitumor therapeutic efficacy. *Proc Natl Acad Sci USA* 1991;**88**:1460–4
- Allen TM, Mehra TC, Hansen B, Chin C. Stealth liposomes: An improved sustained release system for L-D-arabinofuranosylcytosine. *Cancer Res* 1992;**52**: 2431–9
- Allen TM, Hansen CB, Lopes de Menezes DE. Pharmacokinetics of long circulating liposomes. *Adv Drug Del Rev* 1995;**16**: 267–84
- Reddy MS, Raghavendra R, Nayak UY, Kumar AR, Deshpande PB, Dave N. PEGylated liposomes of anastrozole for long-term treatment of breast cancer: In vitro and in vivo evaluation. *J Liposome Res* 2015;**8**:1–19
- Li M, Xiong F, Shi F, Wu S Y, Wu D, Dou J. Homoharringtonine delivered by high proportion PEG of long-circulating liposomes inhibits RPMI8226 multiple myeloma cells *in vitro* and *in vivo*. *Am J Transl Res* 2016;**8**:1355–68
- Shi C, Cao H, He W, Gao F, Liu Y, Yin L. Novel drug delivery liposomes targeted with a fully human anti-VEGF165 monoclonal antibody show superior antitumor efficacy *in vivo*. *Biomed Pharmacother* 2015;**73**:48–57
- Yang C, Xiong F, Wang J, Dou J, Chen J, Chen D. Anti-ABCG2 monoclonal antibody in combination with paclitaxel nanoparticles against cancer stem-like cell activity in multiple myeloma. *Nanomedicine* 2014;**9**:45–60
- Yang C, Xiong F, He X, Song L, Zhan X, Zhang Y, Dou J.  $\gamma$ -Fe<sub>2</sub>O<sub>3</sub> Nanoparticles increase the therapeutic efficacy of combination with paclitaxel and Anti-ABCG2 monoclonal antibody on multiple myeloma cancer stem cells in mouse model. *J Biomed Nanotechnol* 2014;**10**:336–44
- Shi F, Yang F, He X, Zhang Y, Wu S, Li M. Inhibitory effect of epirubicin-loaded lipid microbubbles with conjugated anti-ABCG2 antibody combined with therapeutic ultrasound on multiple myeloma cancer stem cells. *J Drug Target* 2016;**24**:34–46
- Sun WL, Chen J, Wang YP, Zhang H. Autophagy protects breast cancer cells from epirubicin-induced apoptosis and facilitates epirubicin-resistance development. *Autophagy* 2011;**7**:1035–44
- Asharani PV, Low Kah Mun G, Hande MP, Valiyaveetil S. Cytotoxicity and genotoxicity of silver nanoparticles in human cells. *ACS Nano* 2009;**3**:279–90
- Deweerd S. Animal models: towards a myeloma mouse. *Nature* 2011;**480**:S38–9
- Bonnin P, Sabaa N, Flamant M, Debbabi H, Tharaux PL. Ultrasound imaging of renal vaso-occlusive events in transgenic sickle mice exposed to hypoxic stress. *Ultrasound Med Biol* 2008;**34**:1076–84
- Wang X, Zhao F, Shi F, He X, Pan M, Wu D. Reinforcing B16F10/GPI-IL-21 vaccine efficacy against melanoma by injecting mice with shZEB1 plasmid or miR200c agomir. *Biomed Pharmacother* 2016;**80**:136–44
- Dou J, Ni Y, He X, Wu D, Li M, Wu S. Decreasing lncRNA HOTAIR expression inhibits human colorectal cancer stem cells. *Am J Transl Res* 2016;**8**:98–108



33. Tinel A, Tschopp J. The PIDDosome, a protein complex implicated in activation of caspase-2 in response to genotoxic stress. *Science* 2004;**304**:843–6
34. Kasibhatla S, Jessen KA, Maliartchouk S, Wang JY, English NM, Drewe J. A role for transferrin receptor in triggering apoptosis when targeted with gambogic acid. *Proc Natl Acad Sci USA* 2005;**102**:12095–100
35. Martino M, Recchia AG, Vigna E, Morabito L, Morabito F. Sorafenib for the treatment of multiple myeloma. *Gentile Expert Opin Invest Drugs* 2016;**25**:743–9

(Received August 29, 2016, Accepted November 14, 2016)